Wind Energy

WILEY

RESEARCH ARTICLE OPEN ACCESS

Life Cycle Assessment of Additively Manufactured Foundations for Ultratall Wind Turbine Towers

Kathryn E. S. Jones[1] | Mo Li[1,2]

[1]Department of Civil and Environmental Engineering, University of California, Irvine, Irvine, California, USA | [2]Department of Materials Science and Engineering, University of California, Irvine, Irvine, California, USA

Correspondence: Mo Li (moli@uci.edu)

Received: 29 October 2023 | **Revised:** 11 May 2024 | **Accepted:** 25 July 2024

Funding: This work was supported by California Energy Commission (No. EPC-19-007) and the US Department of Education GAANN Fellowship Program.

Keywords: 3D printing | CO_2 emissions | concrete additive manufacturing | concrete foundation | life cycle assessment | wind turbines

ABSTRACT

Wind energy production is rapidly growing in the United States and is expected to continue increasing as more and larger wind turbines are installed. To support these taller and heavier onshore turbines, new foundations must be designed and manufactured. One proposed method of reducing the total amount of concrete and steel in spread foundations is to utilize additive manufacturing to enable more material-efficient designs. To compare these additively manufacturing-enabled designs to conventional foundation designs, this study performs a life cycle impact assessment of four ultra-tall wind turbine foundations: two foundations using 78-MPa 3D printed stay-in-place concrete formwork cast with 35-MPa ready-mix concrete with reinforcements, and two conventional foundations cast entirely out of 35-MPa concrete with reinforcements. The life cycle assessment investigates the environmental impacts of four different stages, including materials production, transportation, construction, and end-of-life. The materials production stage is found to dominate the life cycle results, contributing over 97% of the total CO_2 emissions and over 88% of the fossil fuel depletion for each foundation. Compared to the conventional designs, the Short Flat Ribbed Beam foundation with 3D printed formwork has 22.4% lower CO_2 emissions and 28.3% lower fossil fuel depletion than the Circular foundation, and 2.0% higher CO_2 and 5.9% lower fossil fuel depletion compared to the Tapered foundation. Parametric studies indicate that reducing cement content and increasing recycled content in printed concrete can significantly reduce the overall life cycle impacts of the foundations.

1 | Introduction

The replacement of fossil fuels with renewable energy has become a driving focus in the global effort to mitigate the effects of climate change, as fossil fuel usage remains the single largest emitter of greenhouse gasses globally [1–3]. Wind power is among the largest generators of renewable energy, and within the United States, wind energy has been steadily growing in usage. In 2018, wind energy accounted for 6.5% of US electricity production [4], which increased to 10% of total electricity generation in 2022 [5]. This increasing trend is expected to continue as more onshore and offshore wind farms continue to come online and as more advanced turbines are introduced to the market [6]. With the expanded incentives for renewable energy growth from the Inflation Reduction Act, it is projected that by 2027, US wind energy capacity will grow annually by up to 18.4–22.7 GW [5].

As demand for wind power grows, turbine systems are scaling up to meet it, with research showing that taller wind turbines that can access stronger and more consistent winds will generate greater power [7, 8]. As a demonstration of this relationship, in the United States, the average rated turbine capacity in 2022

was 3.2 MW and the average tower height was 98.1 m, a 7% and 4% increase, respectively, from 2021 and a substantial 350% and 73% increase since 1998–1999 [5]. Continuing this trend, if an onshore wind turbines were to reach a hub height of 140 m or beyond, it would be able to access stronger and more consistent winds that could increase the amount of energy produced at a site with moderate wind shear by over 20% [9], with the potential for development in all 50 US states [10]. Offshore wind turbine towers have already reached a global average hub height greater than 100 m and announced projects past 2025 have heights extending beyond 150 m [11].

When scaling up an onshore turbine to reach these ultra-tall heights of 140 m and beyond, the designs of each subassembly must be updated, including the tower and foundation. Traditional foundations for onshore wind turbines include rock-anchored foundations, pier deep foundations, and spread footings [12, 13], with the spread footing design being the most common among onshore wind turbines. However, spread footing foundations rely on a substantial amount of reinforced concrete to keep the tower from overturning. Both concrete and steel production significantly contribute to anthropogenic carbon emissions. Producing 1 t of cement, the primary ingredient in concrete, generates approximately 1 t of CO_2, while producing 1 t of steel generates around 1.9 t of CO_2 [14, 15]. Therefore, foundation designs that can support an ultra-tall wind turbine tower while using less concrete would reduce the overall carbon impacts of the wind turbine system.

Concrete additive manufacturing, also referred to as 3D concrete printing (3DCP), is an emerging manufacturing method that enables the rapid on-site manufacturing of large-scale, complex turbine foundation formworks. In this approach, a gantry printer is installed above the site location of the foundation and is used to create a concrete stay-in-place formwork by depositing printed concrete material layer-by-layer. The printed formwork can then be installed with rebar and filled in cast concrete before being backfilled with soil prior to the turbine tower assembly. 3DCP eliminates the need for building cumbersome formworks made of wood, reduces labor, and allows for on-site and automated construction using local concrete ingredients, which can be tailored to create printable concrete mixtures that meet specific rheological, mechanical, or environmental demands [16–20]. Incorporating recycled aggregates into 3D printed concrete structures can also reduce their environmental impacts, as seen in prior life cycle assessments (LCAs) [17, 21–23]. 3D printed concrete formworks have been used in previous structural experiments and engineering models [23–27] where they not only improve manufacturing efficiency but also allow novel, optimized geometric designs of foundations to reduce total volume of materials. In order to properly predict the potential life cycle environmental impacts of adopting this novel approach and to identify future paths to reducing the environmental impacts of large-scale wind turbine foundations, a life cycle environmental assessment on different foundation designs is needed.

LCA is a method of evaluating and comparing the environmental impacts of different processes or products. While wind turbine foundations have been modeled in previous LCA studies, it is often only as a complimentary component modeled to match the tower subassembly, with the foundations using the same design method [28, 29]. In these life cycle studies, tower designs vary, but the foundation designs remain consistent, with only dimensions scaled to match the specific tower or seismic loading cases. For example, the life cycle study by Gervásio et al. [30] emphasized the impact of seismic foundation design on LCA results, noting that seismic loading increased the foundation mass by up to 75% for concrete towers. However, the study only considered hexagonal foundations of varying sizes, without examining different types of spread foundations, such as tapered, circular, or other complex geometries. While this approach contributes to understanding a foundation's role in the total environmental impact of a wind turbine, it does not provide insight into how different foundation designs compare environmentally. The concrete foundation is also often presumed to remain in the ground and is excluded from end-of-life measurements [30–33], resulting in a lack of knowledge on how much if any environmental offsets could be achieved by excavating and recycling the concrete foundations.

The LCA conducted in this study quantifies the total life cycle environmental impacts of spread footing concrete foundations made to support a 140-m concrete tower and designed using 3D printed formwork, compared with conventional concrete foundations designed to satisfy identical load cases. Two designs utilizing 3D printed concrete formworks were considered in the study: (1) the initial foundation design that first satisfied the design requirements and (2) the refined foundation design that minimized material mass while satisfying the design requirements. For the conventional foundations, two different designs were considered: (1) a conventional circular slab foundation and (2) a conventional tapered foundation. This study compares the four concrete foundations across each of their life cycle stages, including material production, transportation, construction, and end-of-life decommissioning. A parametric study is conducted to investigate the sensitivity of the LCA results to variations in the initial assumptions. Finally, the concrete foundation results are combined with the results from a prior 140-m-tall turbine tower LCA [23] to create a comprehensive overview of the life cycle impacts of a 140-m-tall novel wind turbine manufactured utilizing concrete additive manufacturing technology.

2 | State of the Art of Land-Based Wind Turbine Foundations

Traditionally, onshore wind turbines use one of the three types of foundations: (1) anchored foundation, (2) piled or pier deep foundation, or (3) spread or spread footing foundation. The choice between which foundation to use is often determined by soil characteristics at the turbine site location [12, 13]. Anchored foundations can be used when competent rock is near the surface of the build site and are comprised of a small foundation pad secured to the rock using prestressed rock anchors. Pier-type deep foundations are used when soil can provide enough lateral resistance to resist overturning and are comprised of solid or hollow cylinders inserted into the ground. Finally, spread foundations are used in strong and stiff moraine soils and are comprised of a slab of reinforced concrete in an octagonal, square, or circular shape that acts as a gravity support to prevent tower overturning. If a spread foundation requires additional support, soil stabilization processes can be used to strengthen the soil such as

jet grouting, or deep piles can be used to transfer loads to deeper bedrock or soil layers [13]. Within this study, spread foundations have been selected based on the site location soil conditions detailed in Section 3.1.

Of the two traditional spread foundations considered in this study, the Conventional Circular foundation is a basic circular slab design commonly utilized in the construction of large towers such as wind turbines towers or grain silos [34, 35] and consists of a single circular mat of reinforced concrete. The Conventional Tapered design is another common foundation used for onshore wind turbines [36] and consists of a circular base that tapers into a smaller upper diameter where the tower mounting is placed. Images of both conventional foundations can be seen in Figure 1.

One unconventional approach to onshore wind turbine foundations is a tree-inspired foundation made of folded steel. This design is comprised of several long pieces of triangular steel that are folded using robotic arms into three-dimensional beams that are then twisted and bound together to form the finished foundation. The primary advantage of this design is being able to use recycled steel instead of concrete, which the manufacturer, STILFOLD, has predicted could lower the CO_2 equivalent emissions of a turbine system by up to 80% [38]. The primary limitation of this design is the challenging construction and manufacturing process, as well as a lack of knowledge concerning if this design could support an ultratall tower.

Another new approach to wind turbine foundations is to use precast concrete components rather than cast the concrete on-site. For this manufacturing method, the foundation is constructed using precast concrete components that are shipped to the tower erection site from the offsite plant. This method circumvents curing issues related to weather or temperature variations at the build-site. Also, the precast concrete foundations are designed to be more easily dismantled than traditionally field cast foundations. Because the foundations are precast and assembled in pieces, those components can be precast using ribs that reduce total concrete mass. Precast foundations made by Anker Foundations for onshore wind turbines have been mass produced and used in Europe since 2020 [39].

Concrete additive manufacturing is a novel construction method for concrete spread foundations focused on in this study. Rather than using wood formworks, the concrete formworks are additively manufactured on-site on top of a precast concrete mat using a gantry 3D printer. Rebars are then installed in the 3D printed concrete formworks. Ready-mix concrete is then cast into the formworks to complete the foundation. Large-scale structural testing of reinforced concrete components made using stay-in-place 3D printed formworks was conducted at the University of California, Irvine to evaluate and validate the manufacturing efficiency and structural capacity. The results showed that the 3D printed thin-wall formworks made of high-strength concrete developed sufficient strength and stability within the initial 48 h to support the weight of the casting concrete, accelerating

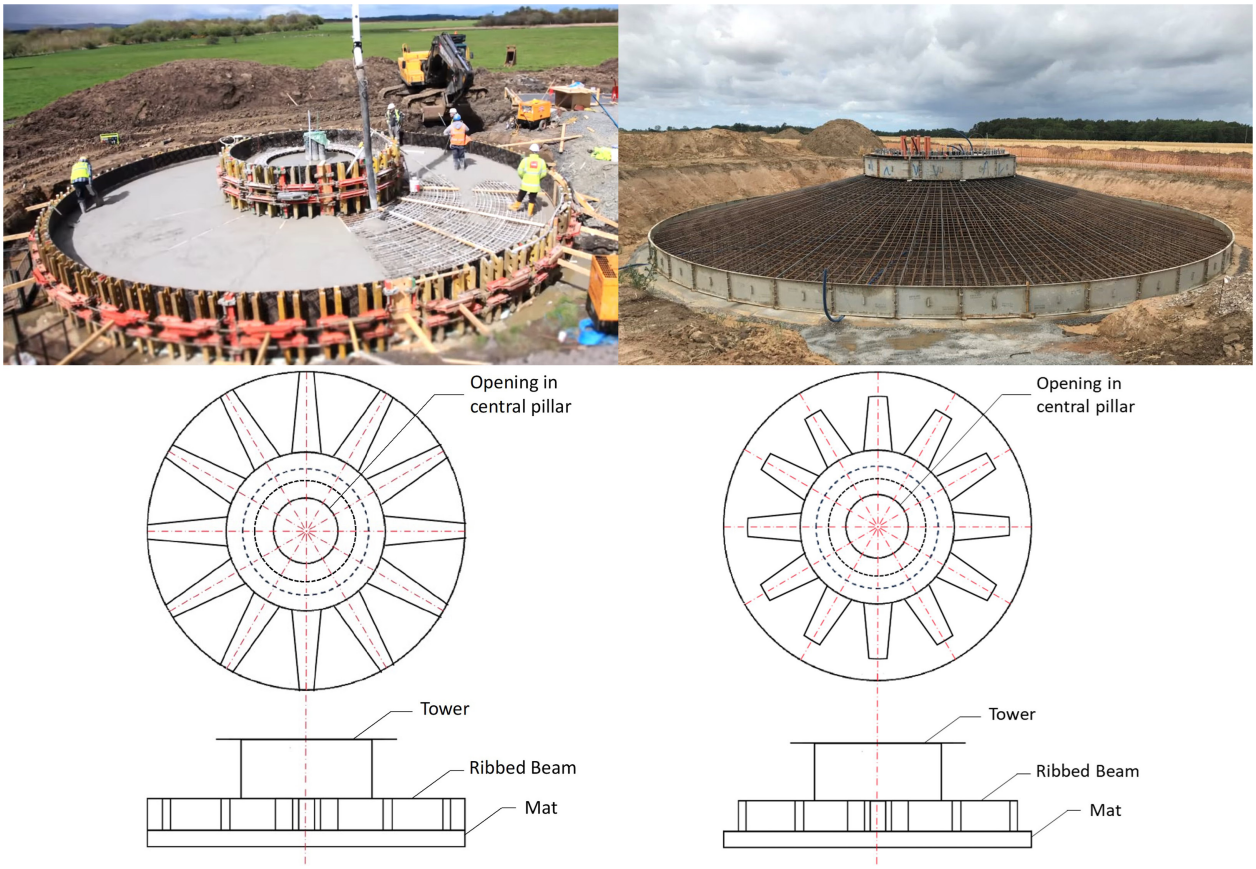

FIGURE 1 | Images of the four foundation designs considered in this study. Clockwise from top left, a Conventional Circular foundation [35], a Conventional Tapered foundation [36], the 3DCP Short Flat Ribbed Beam foundation, and the 3DCP Flat Ribbed Beam foundation [37].

the additive manufacturing process of structural components. Structural components, such as 4-m-tall reinforced concrete columns designed and manufactured using this 3D printing and casting process, were able to withstand both service and extreme (e.g., seismic) loading conditions. Figure 1 shows the 3D cast concrete foundations designed by RCAM and WSP [37] alongside the two conventional designs.

3 | Model for LCA

3.1 | Structural Designs of Concrete Wind Turbine Foundations

Within this study, four concrete foundations were designed to satisfy the strength, stability, and soil-bearing capacity requirements of supporting a novel 140-m-tall 7.5-MW concrete wind turbine. The four foundations include two conventional designs, (1) Conventional Circular foundation and (2) Conventional Tapered foundation, and two designs utilizing 3D printed concrete formwork, (3) 3DCP Flat Ribbed Beam foundation and (4) 3DCP Short Flat Ribbed Beam foundation.

All four tower foundations were designed to support an identical concrete turbine tower with its model shown in Figure 2. To estimate loads, the tower design was adapted from the early concepts of the 140-m-tall 7.5-MW 78-MPa 3D printed concrete tower discussed in the companion tower LCA paper [23]. An additional 4169-kN load was added to the tower dead load to simulate the hub and blades, resulting in a total axial load of 64,207 kN and moment of 709,255 kN·m acting on the foundations.

In addition to the applied loading conditions, the soil-bearing capacity was also considered when designing the footing sizes of the foundations. The soil properties used for each design were based on the construction site location of San Gorgonio near Palm Springs, California, as shown in Table 1. This location was chosen for its existing wind power infrastructure and capacity, along with its proximity to industrial and staffing resources. $\boldsymbol{\gamma}$ represents the density of the soil, $\mathbf{G_s}$ the soil shear modulus, $\mathbf{c}$ the cohesion, $\boldsymbol{\nu}$ the soil Poisson's ratio, and $\boldsymbol{\delta}$ the interfacial friction angle. For this location, the soil is categorized as coarse to medium sand, with little gravel.

The ultimate bearing capacity of the soil was calculated using a safety factor of 2.5, which was selected based on engineering judgment and guidelines from Bowles [40].

Finally, all foundation designs had to meet the strength and stability requirements of reinforced concrete laid out in ACI-318 design code [41]. Both seismic + operating and gravity + operating load types were considered during the design process, with the seismic load case governing the final foundation designs [37].

Each of the foundations and concrete formworks is considered to be constructed/printed on-site at the location where the turbine will be erected. It is assumed that prior to foundation construction, the ground will be excavated to a depth of 6 m and a diameter of 36.5 m, and the bottom 152 mm of the excavation will be filled with either gravel or plain cement to create a flat surface

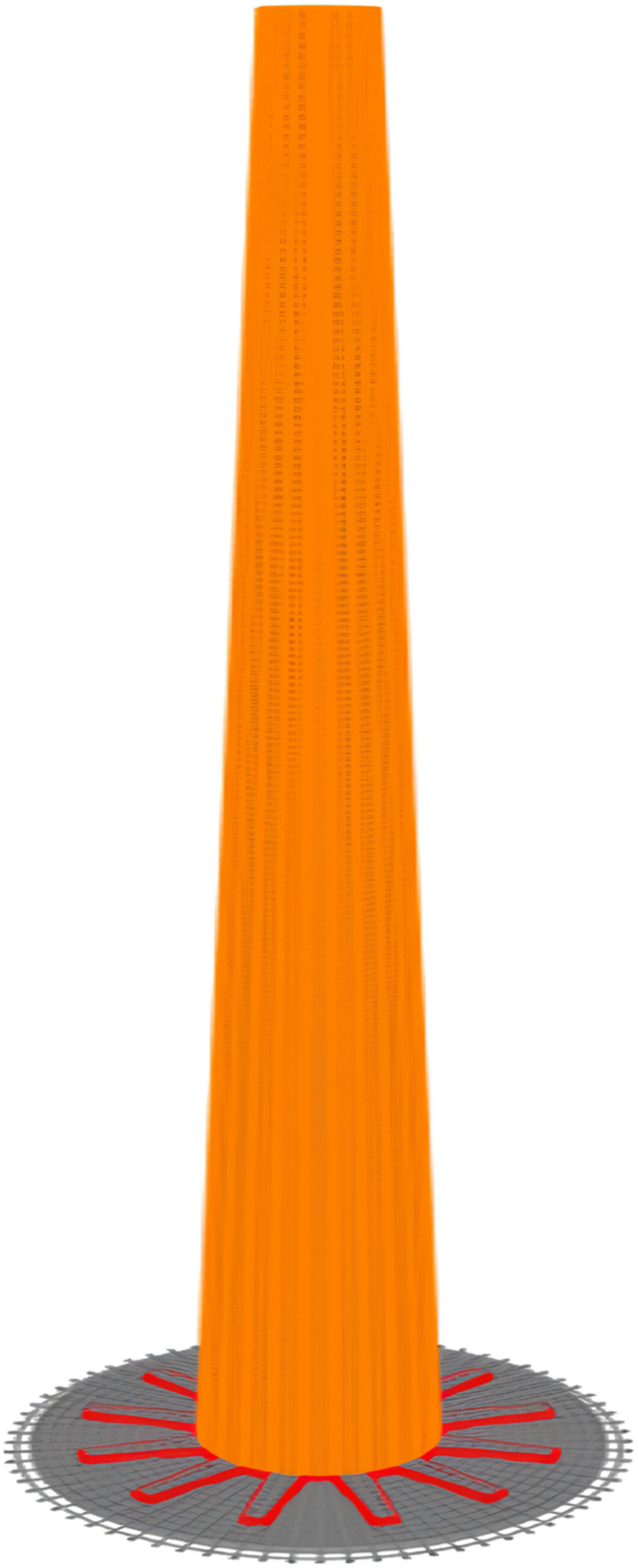

FIGURE 2 | The model of a 140-m-tall wind turbine tower on top of the 3DCP Short Flat Ribbed Beam foundation [37].

TABLE 1 | Soil properties of Palm Springs, California.

γ	G_s	c	ν	δ
18.85 kN/m^3	18,410 kN/m^2	0	0.3	20

TABLE 2 | Design results for concrete foundations.

	3D Cast foundations		Conventional foundations	
Foundation type	**3DCP Short Flat Ribbed Beam**	**3DCP Flat Ribbed Beam**	**Conventional Tapered**	**Conventional Circular**
D_{raft} (m)	30.48	30.48	30.48	30.48
T_{raft} (m)	0.91	0.91	0.91	1.83
# of rib beams	12	12	—	—
W_{rib_avg} (m)	1.22	1.22	—	—
L_{rib_beam} (m)	6.1	9.14	—	—
D_{rib_beam} (m)	0.91	0.91	—	—
$D_{out\_pedestal}$ (m)	12.19	12.19	—	—
$D_{in\_pedestal}$ (m)	6.1	6.1	—	—
D_{raft_top} (m)	—	—	12.19	—
H (m)	—	—	0.91	—
Volume of 3D printed concrete (m^3)	161	203	0	0
Volume of ready-mix concrete (m^3)	667	667	1015	1334
Mass of #4 and #7 rebar (metric ton)	50	52	55	80

Note: Relevant dimensions of the 3DCP Flat Ribbed Beam foundation are shown in Figure A1.

for working. All cast portions of the concrete foundations are designed using normal-strength concrete with compressive strength of 35 MPa, while all printed concrete formworks are assumed to be additively manufactured using high-strength concrete with compressive strength of 78 MPa. High-strength concrete was selected for 3D printing the thin-wall formworks to ensure they develop sufficient initial strength to withstand the 3D casting process and to reduce the total amount of printed material, thereby shortening the overall construction time and potentially reducing costs. The 3DCP formworks will be printed directly on to the base mat of the foundation and will have rebar installed prior to final stay-in-place pouring.

Based on the design requirements, all four modeled foundations utilize a maximum 30.48-m-diameter footprint. The conventional circular foundation is designed with a single uniform slab thickness, while the conventional tapered foundation is divided into two stages; the bottom half of its height is a uniform diameter slab, and the top half of its total height has a linear transition from the base diameter to the final top diameter of 12.19 m. The final design measurements for both conventional foundations are listed in Table 2.

The foundations incorporating 3DCP discussed in this study are made up of four primary elements: (1) a bottom circular mat foundation, (2) flat trapezoidal rib beams, (3) a hollow center pedestal, and (4) 3D printed 152-mm-thick concrete formworks surrounding the rib beams and center pedestal. These designs take advantage of complex 3D printed formworks to reduce overall concrete volume. This is achieved via the rib beams containing and distributing the weight of the backfilled soil to the circular mat foundation, so less overall concrete weight is needed to resist overturning and sliding when compared to the conventional circular and tapered designs. Of the two printed designs, the 3DCP Flat Ribbed Beam foundation was designed first under the assumption that the ribs of the foundation should reach the edge of the circular mat to fully transfer loads between the elements, and was modeled within SAP2000 [42] to ensure it satisfied all foundation design requirements. From this baseline, the design was further refined to reduce the length of the rib beams and the total concrete volume, while still satisfying the stress limitations due to the design loads. The final outcome of this design refinement process is labeled within this study as the 3DCP Short Flat Ribbed Beam foundation, and the complete design for both 3D cast foundations are listed in Table 2. Prior studies [21, 23, 30] have shown that the material phase is the largest contributor to global warming potential (GWP) for large concrete structures, making additional refinement of structural designs a common recommendation to mitigate the environmental impacts of concrete structures. By comparing the 3DCP Short Flat Ribbed Beam against the original 3DCP Flat Ribbed Beam, the environmental impact of this design refinement is quantified within this study.

3.2 | LCA Method

This study is carried out using the "cradle-to-grave" system boundary and includes the phases for material production, transportation, construction, and end of life (recycling and

waste allocation). Figure 3 shows the life cycle phases of a wind turbine foundation considered in this study, and the detailed breakdown of each stage is discussed further in Section 3.3. The use phase is not reported in this study due to the lack of maintenance differences related to any of the modeled wind turbine foundations over the turbine's operating lifespan. The LCA of the foundations described in this study are modeled after the international standards ISO 14040 (2006) and ISO 14044 (2006) [43, 44]. The parameters considered in the LCA include total material volumes and weights, site location, manufacturing method, printing speed, number of workers, construction schedules, and end-of-life recovery percentages.

Since the purpose of this LCA is to highlight the differences between the tower foundations, the life cycle models in this study only consider the systemic differences between the concrete foundations while allowing any shared features (tower fixtures, excavation construction, and roadwork) to remain equivalent and unconsidered within the study. The environmental categories used to quantify the results of the foundation LCA are GWP, eutrophication, smog, fossil fuel depletion, acidification, ozone depletion, carcinogens, noncarcinogens, respiratory effects, and ecotoxicity. Reported units for each environmental indicator are listed in Table 3.

3.3 | LCA Assumptions

The construction process undertaken for each of the concrete foundations is as follows. As detailed in Section 3.1, the site is prepared for each foundation by first clearing the area of vegetation before excavating the ground to a depth of 6 m and a diameter of 36.5 m and then coating the bottom 152 mm of the excavation with a layer of either gravel or cementitious material to create a flat working surface. After the site is prepared, the formwork and rebar cage are installed for the bottom circular mat portion of the foundations. The circular mat foundation is then filled in with 35-MPa ready-mix concrete, poured using either a boom pump or a line pump supplied by ready-mix truck loading material into the pump's hopper. Because all foundations include a base circular mat, the initial stage formwork is not considered in the LCA. For the 3DCP foundations, the next step of the construction process is printing the stay-in-place formwork on top of the circular mat. The formwork is comprised of a 152-mm-thick 78-MPa concrete mixture and is printed using a mobile gantry printer with an assumed printing rate of 3.6 m^3/h. Finally, the rebar is installed into the rib beams and center pedestal as shown in Figure 4 and is then filled with 35-MPa ready-mix concrete using the same process as the circular mat. A JXLRZ 47-5.16 Boom Pump and a 2016 Kenworth W900 Mixing Truck are assumed for all ready-mix concrete pouring, with a pumping rate of 164 m^3/h. These machines are modeled within the life cycle inventory as a high load factor and steady-state machine in the Ecoinvent 3 database, respectively, based on EPA regulations [45]. The last step for each foundation is backfilling with native soil above the foundations and between each of the rib beams for the 3DCP Short Flat Ribbed Beam and 3DCP Flat Ribbed Beam foundations. The number of work hours considered for each part of the construction phase modeled in the LCA is listed in Table 4.

Figure 5 shows the mix proportions of the two types of concrete considered in this study: 78-MPa 3D printed concrete and

TABLE 3 | Environmental indicators for LCA, derived from TRACI impact indicator categories.

Impact indicator	Unit
Ozone layer depletion potential (ODP)	kg CFC-11 equiv.
Global warming potential (GWP)	kg CO_2 equiv.
Acidification potential (AP)	kg SO_2 equiv.
Eutrophication potential (EP)	kg N equiv.
Photochemical smog creation potential (POCP)	kg O_3 equiv.
Fossil fuel depletion (FFD)	MJ surplus
Carcinogenic potential	CTUh
Noncarcinogenic potential	CTUh
Respiratory effect potential	kg PM2.5 equiv.
Ecotoxicity potential	CTUe

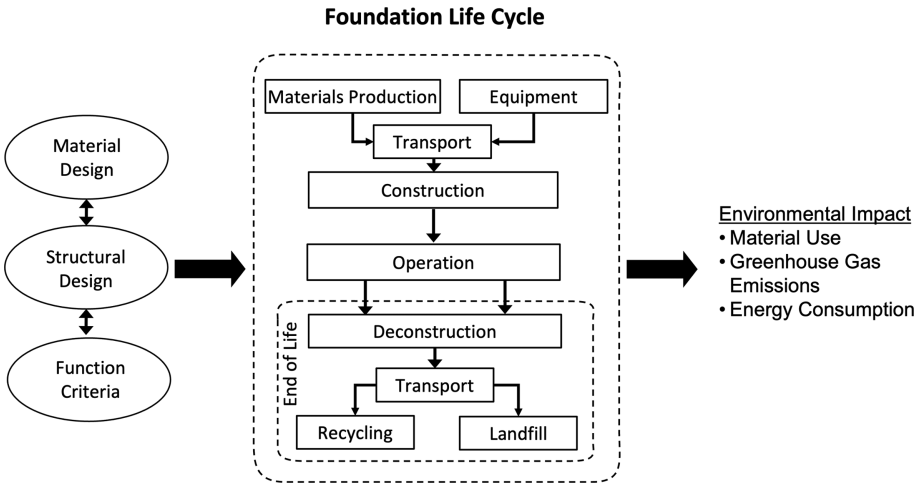

FIGURE 3 | Cradle-to-grave life cycle of a wind turbine foundation.

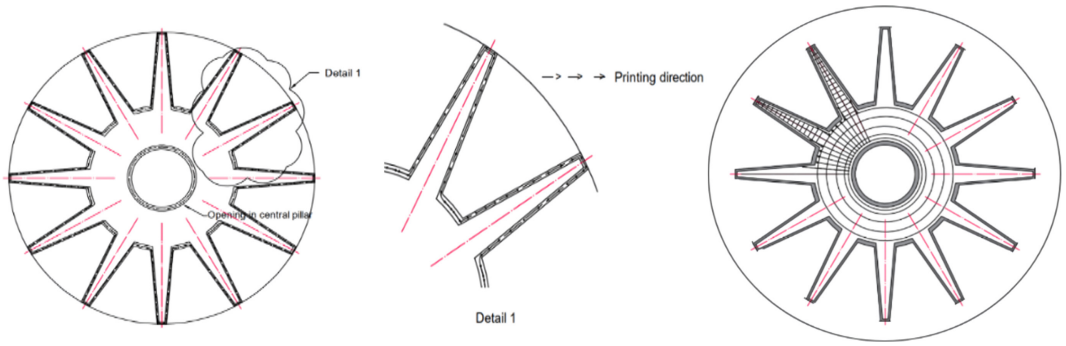

FIGURE 4 | From left to right, the printed formwork of the 3DCP Flat Ribbed Beam foundation, a detailed view of the printing path, and the rebar caging of the 3DCP Short Flat Ribbed Beam foundation [37].

35-MPa ready-mix concrete. As explored in a previous study [23], the high-strength printed concrete has substantially more cement content than the normal-strength concrete, which has a higher water-to-cement ratio and also includes larger aggregates such as gravel. These values are used to calculate the environmental impacts by unit weight of the concrete mixtures using the Ecoinvent 3 [46] material database within the SimaPro software. The impact indicator values for the 35-MPa ready-mix concrete are sourced from the 2020 Environmental Product Declaration (EPD), which summarizes the cradle-to-gate LCA results of 30 ready-mix concrete mixtures from eight Southern California plants. This includes raw material supply, transportation, and manufacturing from the supplier to the concrete producer (gate) [47]. Four life cycle indicator categories (carcinogenic, noncarcinogenic, respiratory effect, and ecotoxicity potential) are not included in the EPD and are instead modeled using the "35 MPa {GLO} market for|APOS, U" Ecoinvent 3 database entry.

The same travel distances and site location used in the LCA of ultra-tall wind turbine towers [22] are used in this study. San Gorgonio near Palm Springs, California, is selected as the wind turbine tower site location, with concrete materials being supplied from a local ready-mix plant 6.5 km from the build site and the remainder of the materials (steel rebar, 3D printers) being sourced 148 km away from the nearby metropolis of Los Angeles.

For the use phase, no considerations are made for the life cycle inventory of the concrete foundations. While some minor maintenance checks of the foundation can be expected over the service life of the turbine, such as annually checking the exposed foundation for cracks or the mounting bolts for rust or damage suggested by the "Strategy for Extending the Useful Lifetime of a Wind Turbine" report by Megavind [48], these checks are assumed to be identical for all four foundations.

For the end-of-life phase, it is assumed that 100% of the foundation will be excavated and crushed prior to shipping 70% of the total mass to a recycling plant (34 km from build site) and the remaining 30% to an inert landfill (24 km from build site). A Screen Machine 5256T Impact Crusher with a 354 kW diesel engine and a crushing rate of 1 m^3 per minute was modeled within the life cycle inventory as a steady-state machine in the Ecoinvent 3 database, based on EPA regulations [45]. This approach represents a more ambitious end-of-life phase than most wind turbine foundations, which are often partially left in place and buried in the ground [49]. By calculating the full amount of reclaimed material, one can estimate what impact indicator values for scenarios where only a portion of the foundation is excavated by multiplying the full reclamation values by the corresponding percentage.

To properly credit the recycled materials within the cumulative LCA results, a credit-buyback system was assumed, where the recycled material is credited as offsetting an equivalent quantity of virgin material used in the material-stage inventory [44]. This method allows the volume of emissions saved by using recycled materials to be counted without overestimating the impact of recycling by excluding the processes needed to create the material. For instance, while steel is fully recyclable, recycled steel does not entirely offset the material processing and transportation initially required to produce the rebar. Two major materials are considered for recycling in this study: concrete and steel. Concrete waste is assumed to be crushed and recycled as coarse aggregates, providing an environmental credit for partially replacing the initial gravel content in the 35-MPa ready-mix concrete mixture. However, recycled aggregates are not credited in the cumulative environmental impacts reported in Section 4. Instead, Section 5's end-of-life parametric study investigates the environmental benefits of recycling concrete. This approach is due to the still-developing understanding of using recycled aggregates in concrete structural designs; previous studies have reported a 10%–20% reduction in compressive strength of concrete when using 100% recycled aggregates [50, 51]. Steel waste is assumed to be recovered and recycled into scrap steel, credited within the life cycle inventory as offsetting the steel used in rebar production. To estimate the percentage by weight of initial scrap steel in the rebar, it was assumed that an electric arc furnace (EAF) process would be used, with the steel containing 90% scrap by volume [52, 53]. While recycled rebars need to be valorized or cleaned prior to reuse, the purification and scrap preparation processes are not currently considered in this study.

4 | LCA Results

The inventory analysis conducted for each concrete foundation scenario was conducted using the SimaPro life cycle assessment (LCA) software, release 9.0.0.49, utilizing the Ecoinvent 3 Version 3.5, Industry data 2.0, and USLCI material databases [46, 54, 55]. The numerical weighting of the impact indicators

TABLE 4 | Foundation LCA variables for transportation, construction, and end-of-life stages.

Category	Variable	Value
General		
	Tower location	San Gorgonio, near Palm Springs, California
Construction		
	Ready-mix location	Robertson's Ready Mix (13990 Apache Trail, Cabazon, California 92230)
	Distance from ready-mix to tower (km)	6.5
	Worker travel distance (km)	11.3
	Clear land	332 person-hours 5 days
	Formwork installation	400 person-hours 3 days
	Pour foundation	300 person-hours 1 day
	3D print ribbed beams[a]	200 person-hours 2 days
	Rebar cage installation	593 person-hours 3 days
	Pour center pedestal concrete	584 person-hours 2 days
	Backfill with native soil	92 person-hours 1 day
	Concrete pump	JXLRZ 47-5.16
	Pump rate	164 m^3/h
	Pump engine	> 100 HP Hi LF
	Concrete mixer	2016 Kenworth W900 10 × 4 Mixer Truck
	Mixer engine	385 HP SS
	Printing rate	3.6 m^3/h
End of life		
	Landfill location	Burrtec Recovery & Transfer, 70100 Edom Hill Rd, Cathedral City, California 92234
	Dist. from wind farm to landfill (km)	24
	Recycling plant	SA Recycling (29,250 Rio del Sol Rd, Thousand Palms, California 92276)
	Dist. from wind farm to recycling (km)	34
	Crusher	Screen Machine 5256T Impact Crusher
	Crush rate	1 m^3 per minute
	Engine	CAT ACERT C13 475 HP (354 kW) diesel engine
	# workers for concrete crushing	20

[a]Not included for nonprinted foundations.

was performed using the Environmental Protection Agency's Tool for Reduction and Assessment of Chemicals and Other Environmental Impacts (TRACI 2.1 V1.05/US 2008) analysis framework. For each of the four foundation models, the ten impact indicators shown in Table 3 were calculated for each of the life cycle stages (materials, transportation, construction, and end-of-life), with their cumulative totals shown in Figure 6. From these LCA results, we can see that the 3DCP Short Flat Ribbed Beam foundation has the lowest life cycle impact indicator values for smog, fossil fuel depletion, acidification, and carcinogens, while the Conventional Tapered foundation has the lowest global warming, eutrophication, ozone depletion, noncarcinogens, respiratory effects, and ecotoxicity impact indicators. The Conventional Circular foundation exhibits the highest life cycle values for GWP, smog, fossil fuel depletion, acidification, carcinogens, noncarcinogens, respiratory effects, and ecotoxicity, while the 3DCP Flat Ribbed Beam foundation shows the highest ozone depletion and eutrophication values. The environmental impacts and percentage contributions to the cumulative life cycle impact for each foundation's life cycle stages are listed numerically in Appendix Tables A4 and A5. The material stage dominates the total results for all six impact indicators. For GWP, the material stage contributes 97%–98% of the total life cycle impact of each concrete foundation.

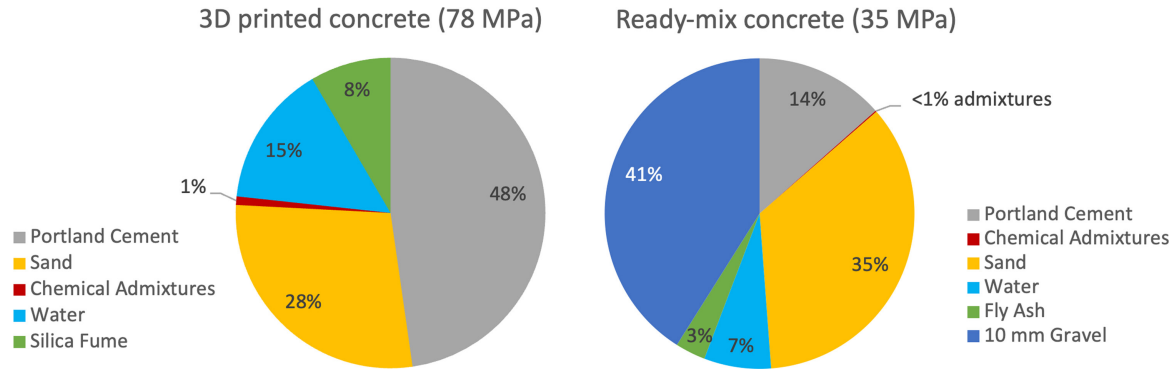

FIGURE 5 | Mix designs of 3D printed concrete and ready-mix concrete with 78 MPa and 35 MPa 28-day compressive strengths, respectively. Percentages of ingredients are based on weight. The mix percentages by weight of the 35-MPa concrete are extrapolated from the "35 MPa {GLO} market for|APOS, U" entry in the Ecoinvent 3 database due to the lack of specific mix design data in the CalPortland EPD [46].

Figure 7 shows a breakdown of the material stage by component. The largest contributor for all four foundations is the 35-MPa cast concrete, followed by the printed 78-MPa concrete for the 3DCP foundations, with the steel rebar being the smallest contributor for each foundation. Although the foundations designed using 3D printed formworks have a lower volume of total concrete than the conventional foundations, the use of the 78-MPa 3D printed concrete results in a total material-stage GWP that is greater than that of the conventional foundations. This difference can be attributed to the comparative GWP emissions of the two different materials, which, in turn, is a result of the cement percentage by weight in the mix designs. The 35-MPa ready-mix concrete is composed of 13.48% cement by weight, while the 78-MPa 3D printed concrete contains 47.73% cement by weight. Calculating the GWP emissions of an equivalent volume of concrete material reveals that 1 m^3 of 78-MPa printed concrete produces nearly three times the kilograms of CO_2 equivalent compared to the 35-MPa ready-mix concrete, as shown in Figure 8. Due to the decrease in printed formwork, the 3DCP Short Flat Ribbed Beam foundation emits 44,725 kg less CO_2 equivalent compared to the 3DCP Flat Ribbed Beam foundation, with over 40,052 kg CO_2 saved purely from the reduction in printed material.

For the transportation stage, the Conventional Circular foundation has the largest life cycle impact across all ten impact indicator categories, approximately 1.3 times greater than the other three foundations. This can be attributed to the material inventory for the Conventional Circular foundation, which required the largest mass of materials, leading to the largest tons-per-kilometer of travel units. The 3DCP Short Flat Ribbed Beam had the smallest transportation-stage emissions in every category except respiratory effects, although the difference was less than 2% compared to the Conventional Tapered foundation. This is because although the 3DCP Short Flat Ribbed Beam foundation has a smaller material mass than the Conventional Tapered foundation, the need to transport the 3D printers to the build site results in minimal difference in transportation-stage life cycle emissions.

For the construction stage, the foundations using 3D printed formworks have approximately 1.3 times the life cycle impacts compared to both conventional foundations from a worker transport perspective. However, when the emissions from pumps and mixers are accounted for, both foundations using 3D printed formworks exhibit 2–27% lower impacts than the conventional foundations in terms of ozone depletion, GWP, smog, acidification, and fossil fuel depletion. The higher worker transport impact for the foundations with 3D printed formworks can be traced back to the additional construction processes required, particularly the printing of the formworks, which was estimated to take 200 person-hours to complete. The construction-stage worker transport emissions for the conventional foundations are likely overestimated, as more backfilling time is needed to carefully fill around the ribbed beams used by the foundations with 3D printed formwork. This may be counteracted by the time spent installing the rebar cages; while conventional foundations require more rebars, the foundations with 3D printed formworks may involve a more complex rebar assembly. Despite the higher worker transport emission, the foundations with 3D printed formworks use less total material than the conventional foundations, resulting in smaller pump and mixer emissions and lower cumulative construction-stage emissions in five out of ten life cycle indicators. Since the construction phase contributes less than 1% to total emissions in each indicator category, additional detailing might be more beneficial for an economic life cycle calculation rather than the environmental LCA considered in this study.

The total impacts of the end-of-life stage generally correspond to the total mass of the foundations, with the heaviest foundation, Conventional Circular foundation, having just over 1.6 times the emissions of the lightest foundation, the 3DCP Short Flat Ribbed Beam foundation. Although the heavier conventional foundations contain more steel rebar and therefore receive more credit from recycling those materials, the additional weight of the materials being transported to the recycling facility or inert landfill, along with the extra time required to fully crush the foundations, outweighs that benefit when compared to the less massive foundations with 3D printed formworks.

5 | Parametric Study

To further expand upon the LCA results and to make predictions for future designs, two parametric studies were carried

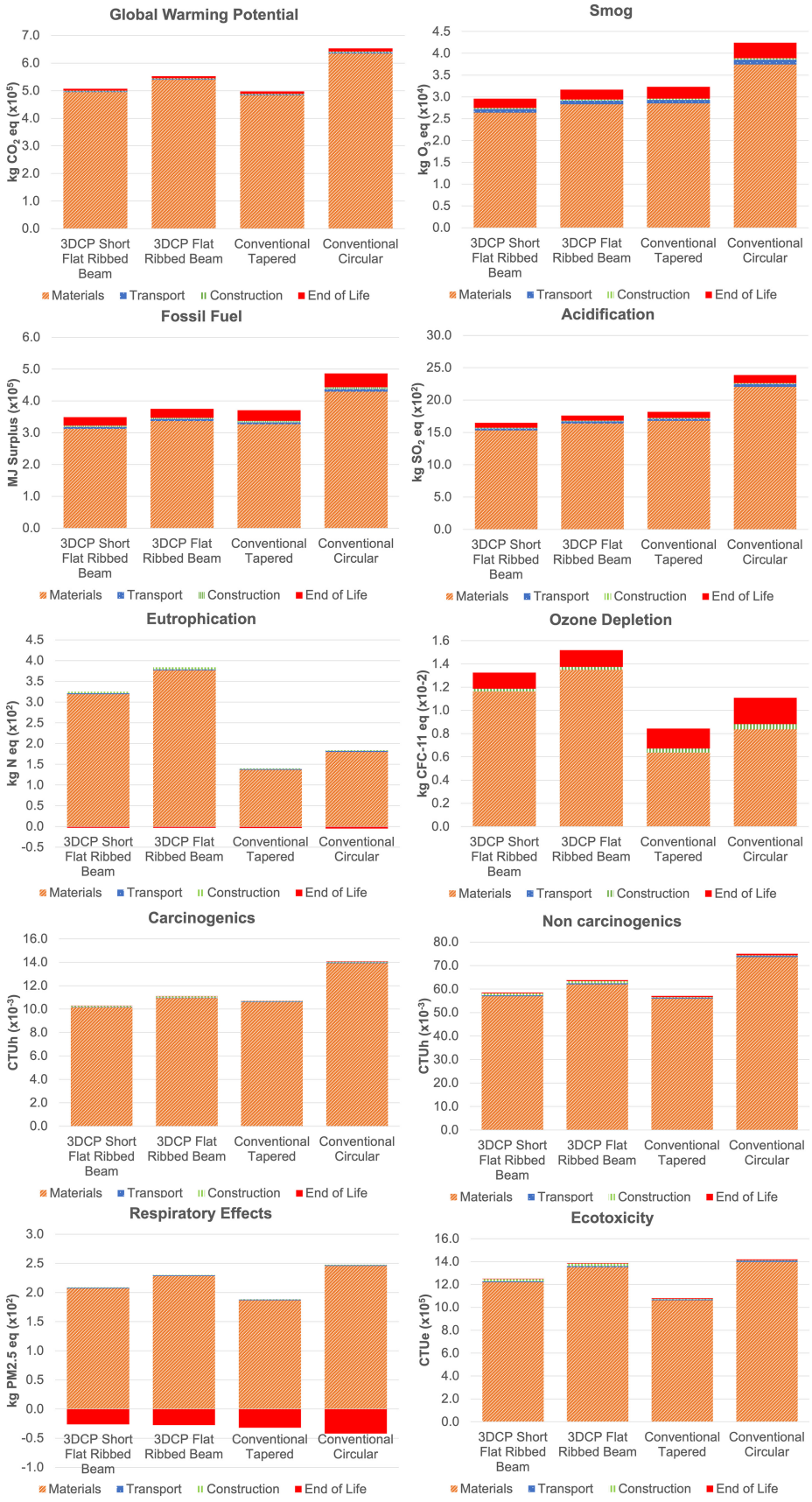

FIGURE 6 | GWP, smog, fossil fuel depletion, acidification, eutrophication, ozone depletion, carcinogenics, noncarcinogenics, respiratory effects, and ecotoxicity impact categories for the Conventional Circular, Circular Tapered, 3DCP Flat Ribbed Beam, and 3DCP Short Flat Ribbed beam wind turbine foundations, broken down by life cycle stage contribution. Numerical values and percentage contribution tables can be found in Appendix Tables A4 and A5.

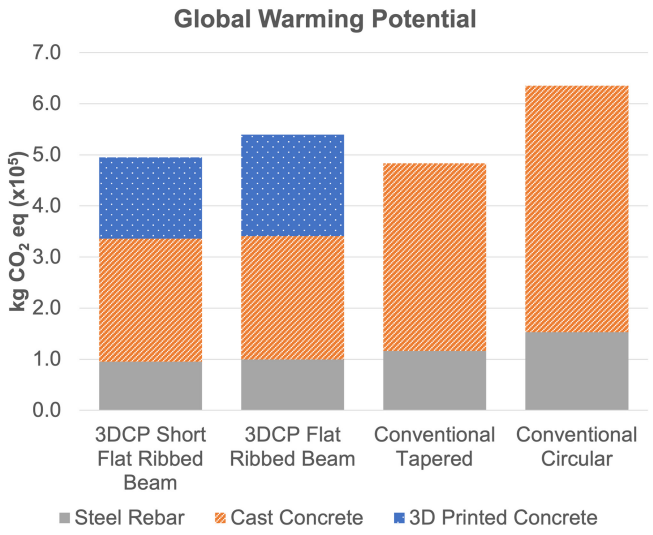

FIGURE 7 | Foundation LCA materials stage breakdown.

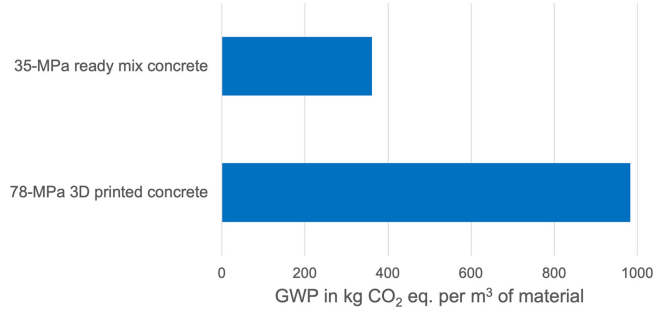

FIGURE 8 | Global warming potential of 1 m^3 of conventional 35-MPa ready-mix concrete compared to 78-MPa printed concrete.

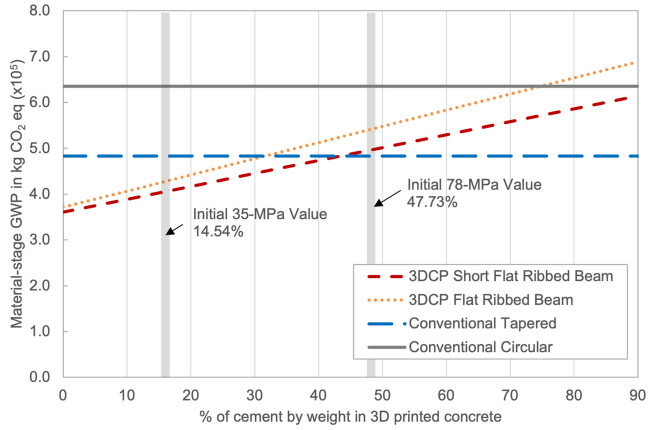

FIGURE 9 | Material-stage parametric study.

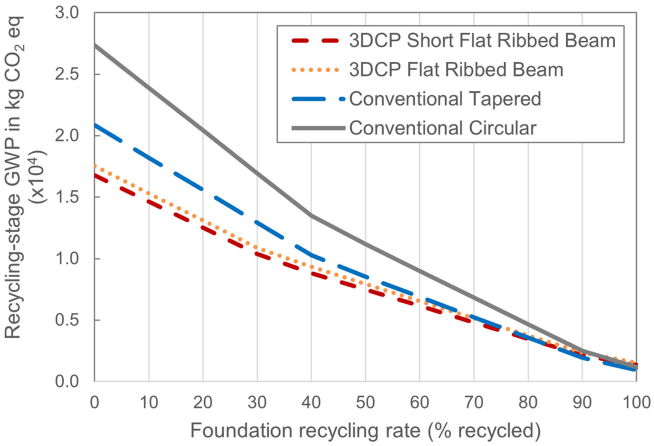

FIGURE 10 | End-of-life-stage parametric study.

out to investigate the effects of key parameter variations on the two life cycle stages with the largest emissions impacts: materials and end-of-life stages. The parameters selected for variation are the percentage of cement by weight in the printed concrete for the materials stage and the recycling rate of the foundation for the end-of-life stage.

As found in the 3DCP wind turbine tower LCA [23] as well as the foundation LCA in this study, the materials stage is the most impactful life cycle stage in terms of cumulative emissions, contributing over 75% to each of the impact indicator categories and over 97% to the GWP of each foundation. The largest contributor to each foundation's material-stage emissions is the concrete, with concrete being the primary source of emissions within each concrete mix design. To investigate the effect of tailoring the 3D printed formwork on the material-stage emissions, the percentage of cement by unit weight in the 78-MPa 3D printed concrete is varied, assuming the total volume and density of the concrete mixture remain constant. As shown in Figure 9, the initial cement percentage in the 78-MPa concrete results in both 3DCP foundations having slightly higher GWP compared to the Conventional Tapered concrete foundation, with the GWP of the 3DCP Flat Ribbed Beam foundation being 11.7% higher and the GWP of the 3DCP Short Flat Ribbed Beam foundation being 2.4% higher. However, if both foundations were to use a cement percentage by weight similar to a 35-MPa 3D printed concrete design, they would both produce fewer kilograms of CO_2 equivalent emissions than the Conventional Tapered foundation: 6.05×10^4 kg less for the 3DCP Flat Ribbed Beam foundation and 8.16×10^4 kg less for the 3DCP Short Flat Ribbed Beam foundation.

For the end-of-life stage, it is assumed that 100% of the foundations are excavated and crushed before being transported either 34 km to a recycling plant or 24 km to an inert landfill. The original study in Section 3 assumed a recycling rate of 70%, with 30% of the material going to inert landfills. In this parametric study, the recycling percentage is varied, as shown in Figure 10. The recycled material is credited back as negative values equivalent to the original material they are offsetting, which is gravel for the recycled concrete and scrap steel for the rebar. Any recycled material that exceeds the mass of original content of gravel or scrap steel is not subtracted from the total emissions, as it would not have been used in the initial construction of the foundations. However, the excess recycled material reduces the total inert landfill emissions, which are calculated based on the weight of disposed material. In this parametric study, it is assumed that 100% of the gravel and scrap steel in the original foundation designs can be replaced with recycled equivalents. However, the effect of recycled coarse aggregates

on concrete material properties is still a subject of ongoing research. Some studies have found a negligible loss in compressive strength even with 100% recycled aggregates [56], while others have noted compressive strength losses of 10%–15% at the same substitution percentage [50]. Therefore, this parametric study may present an optimistic estimate, highlighting the maximum possible environmental offset of recycling concrete materials.

The changing slopes of each foundation's trendline seen in Figure 10 correspond to the percentages by weight of the material being offset. The first change in slope corresponds to the percentage of gravel in the total volume of concrete. Both conventional foundations are made entirely of 35-MPa ready-mix concrete, which has a gravel percentage by weight of 41%, while the 3DCP Short Flat Ribbed Beam and the 3DCP Flat Ribbed Beam have lower gravel percentages by weight of 33% and 31% respectively, due to their inclusion of 3D printed formwork which has no coarse gravel in it. The second change in slope corresponds to the percentage of scrap steel in the rebar. All rebar is assumed to be comprised of 90% scrap steel, so all four foundations have a slight decrease in slope past a 90% recycling rate. The magnitude of the slope corresponds to the original mass of the foundation, with larger masses benefitting more from a larger recycling rate.

6 | Discussion

From the results of this LCA study, the 3DCP Short Flat Ribbed Beam concrete foundation has the lowest life cycle emissions in terms of smog, fossil fuel depletion, acidification, and carcinogens compared to other concrete foundations. However, the Conventional Tapered concrete foundation has the lowest emissions in terms of GWP, ozone depletion, eutrophication, noncarcinogens, respiratory effects, and ecotoxicity. The smog, fossil fuel depletion, and acidification categories show relatively larger contributions from the transportation and end-of-life stages than the other categories, depending on where the mass of the foundations is transported to and from the final site. The 3DCP Short Flat Ribbed Beam foundation has the lowest total foundation mass, resulting in the lowest emissions in these categories. However, while the transportation and end-of-life stages also significantly impact the ozone depletion and respiratory effects categories, these differences are outweighed by the emissions associated with the high-strength printed concrete, which are highest for the 3DCP Short Flat Ribbed Beam foundation design. The remaining five categories, GWP, eutrophication, carcinogens, noncarcinogens, and ecotoxicity, are predominantly driven by the materials stage. As seen in Figure 8, the 78-MPa 3D printed concrete has 2.7 times GWP emissions per unit volume compared to the 35-MPa ready-mix concrete. Thus, even though the 3DCP Short Flat Ribbed Beam foundation is 19.8% lighter than the Conventional Tapered foundation, its material-stage GWP is 2.4% higher. The results also reveal that, because the 3DCP Short Flat Ribbed Beam foundation contains less steel reinforcement than the Conventional Tapered foundation, its material-stage fossil fuel depletion is 4.4% lower. The lighter weight of the 3DCP Short Flat Ribbed Beam foundation further reduces the fossile fuel depletion in the transportation, construction, and end-of-life stages. Consequently, the total life cycle GWP of the 3DCP Short Flat Ribbed Beam foundation is 2.0% higher, while its life cycle fossil fuel depletion is 5.9% lower than that of Conventional Tapered foundation.

Between the two 3DCP foundations, the 3DCP Short Flat Ribbed Beam foudation has 6%–15% lower emissions across all impact indicator categories, with an 8.2% lower GWP, representing 45,194 kg less of CO_2 equivalent. This result highlights the substantial evnironmental benefits that additional engineering refinement can provide for wind turbine foundation designs, beyond only economic cost saving. The material-stage and end-of-life-stage parametric studies indicate further opportunities for emission-reducing refinements of concrete foundations. The design change with the greatest potential GWP impact is reducing the cement content in the final design, which can be achieved either by reducing the cement content in the printed material itself or by reducing the total amount of printed concrete material. The 78-MPa 3D printed concrete emits 983 kg CO_2 equivalent per m^3 of material, while an equivalent volume of 35-MPa 3D printed concrete emits only 405 kg CO_2 equivalent [23]. If the 3D printed formwork is made of 35-MPa printed concrete rather than the 78-MPa printed concrete, the life cycle GWP emissions of the 3DCP ShortFlat Ribbed Beam foundation could be reduced by 22.5%. Given that the 35-MPa printed concrete has a lower compressive strength than the 78-MPa concrete, the initial 152-mm formwork thickness might need to increased. As an alternative to changing the printed concrete material, emissions can be lowered by redesigning the foundations to require less 3D printed formworks. One opportunity for improvement could involve using a tapered circular mat rather than the current flat circular mat, and employing six-axis robotic printers to create formwork directly on the sloped surface [57]. Additionally, more variables beyond the length of the foundation ribs could be investigated, perhaps with the use of advanced generative design software [58].

Further research into the LCA of wind turbines and their foundations should also consider other modern foundation designs, such as common octagonal spread footing foundations, and a more comprehensive pairing of novel tower and foundation designs such as precast and steel foundations. Future work should also consider the impact of recycling foundations at different excavation maximums rather than assuming a complete removal of the foundation, as many site locations only require the top 1–1.5 m of material to be cleared [49].

6.1 | 7.5-MW Ultratall Wind Turbine Potential

To provide a complete estimate of the life cycle impacts of a fully assembled 140-m-tall 7.5-MW wind turbine system, the GWP emissions of the four concrete foundation designs evaluated in this study are combined with the four turbine towers assessed in a previous study [23]. These are further coupled with the estimates for the tower nacelle, blade, and hub subassemblies sourced from the NREL 5-MW reference wind turbine [59], with a material inventory reported by Raadal et al. [60], as recreated in Table A6. Additional transportation values for the nacelle/blade/hub subassemblies are estimated in SimaPro, assuming the materials will be transported from the same wind turbine

TABLE 5 | Summarized global warming potential of tower and foundation combinations in grams of CO_2 equivalent per kilowatt-hour (kWh) assuming a 45.5% capacity.

	Tower			
Foundation	**35-MPa Printed**	**78-MPa Printed**	**78-MPa Cast**	**Steel**
3DCP Short Flat Ribbed Beam	5.23	6.51	6.05	6.00
3DCP Flat Ribbed Beam	5.29	6.57	6.11	6.06
Conventional Tapered	**5.22**	6.50	6.04	5.99
Conventional Circular	5.43	**6.71**	6.25	6.20

Note: Highest and lowest values are in bold.

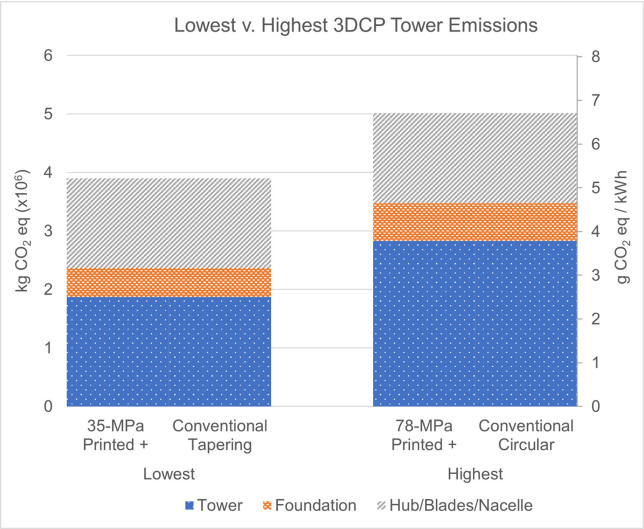

FIGURE 11 | Lowest and highest tower and foundation combinations with respect to global warming potential (GWP) and grams of CO_2 equivalent per kilowatt-hour (kWh). This estimate does not include shared features for the tower and foundation subassemblies.

assembly plant in Pueblo, Colorado, as the steel tower. The original inventory of the rotor and nacelle is derived from a 5-MW offshore turbine and is therefore likely an unconservative estimate for a true 7.5-MW onshore turbine. The concrete foundations in this study were also modeled based on the load cases of the original 78-MPa printed tower design, and therefore may vary slightly if adjusted for the other three tower models. For example, the more massive 35-MPa printed tower might require a less massive foundation due to its higher dead load, while the lighter tubular steel tower may need a more massive foundation to prevent overturning. These totals also do not account for shared features that were omitted from the tower and foundation LCAs, such as excavation, road work, and tower/foundation connecting features.

All of the tower and foundation combinations are shown in Table 5 in terms of total grams of CO_2 per kilowatt-hour, assuming the 7.5-MW turbines operate for 25 years at 45.5% capacity, as calculated using the SAM tool from the U.S. National Renewable Energy Labortory (NREL) for a 140-m hub height at the Palm Springs site location [61]. It is assumed that the nacelle/blade/hub subassemblies are identical for each foundation/tower combination and are treated as a constant value.

Figure 11 shows both the lowest GWP combination, consisting of the 35-MPa 3D printed concrete tower plus the Conventional Tapered concrete foundation, and the highest GWP combination, consisting of the 78-MPa 3D printed concrete tower plus the Conventional Circular concrete foundation. While the GWP of the Conventional Tapered foundation is 1.9% lower than the 3DCP Short Flat Ribbed Beam foundation, this amounts to a nearly negligible difference of 0.01 g CO_2/kWh in Table 5. This indicates that, from a GWP perspective, 3DCP foundations are comparably viable to the conventional alternatives.

7 | Conclusions

In this study, four concrete foundations designed to support a 140-m-tall wind turbine tower, two concrete foundations using 3D printed concrete formworks and two conventional concrete foundations, were compared using a life cycle impact assessment (LCA) framework.

The LCA results shows that, compared to the Conventional Tapered foundation, the 3DCP Short Flat Ribbed Beam foundation has 2.0% higher CO_2-equivalent emissions but 5.9% lower fossil fuel depletion. This difference is relatively minor, given the uncertainty in life cycle inventory data. In contrast, compared to the Conventional Circular foundation, the 3DCP Short Flat Ribbed Beam foundation has 22.4% lower CO_2-equivalent emissions and 28.3% lower fossil fuel depletion.

The material stage is found to dominate the emissions for all four foundations, contributing over 97% to the cumulative global warming potential (GWP) and 88%–90% of the life cycle fossil fuel depletion. This is due to the large volume of materials needed for the foundations. Compared to the environmental impact of the materials, the construction process and worker travel contribute much less to the CO_2 emissions. Cement content in concrete is identified as the largest contributor to material-stage GWP. Although the Conventional Tapered foundation has 24.7% more concrete by mass than the 3DCP Short Flat Ribbed Beam foundation, the latter has higher GWP emissions due to the inclusion of 78-MPa 3D printed concrete, which has 2.7 times the GWP of 35-MPa ready-mix concrete. However, a mere 4.2% decrease in cement content by weight in the 78-MPa 3D printed concrete reduces the CO_2-equivalent emissions of the 3DCP Short Flat Ribbed Beam foundation to below those of the Conventional Tapered foundation, as indicated in the parametric study. This reduction is achievable through the use of coarse

aggregates, waste and recycled ingredients, and supplementary cementitious materials in the 78-MPa 3D printed concrete. Additionally, recycling concrete foundations is shown to reduce environmental impacts compared to landfill alternatives, with larger foundations benefiting more significantly from higher recycling rates. The results of this LCA support ongoing efforts to develop and use 3D printed concrete materials with lower CO_2-equivalent emissions. Furthermore, optimized foundation designs that use less high-cement-content printed concrete will further reduce life cycle environmental impacts, as shown by the 8% decrease in CO_2-equivalent emissions between the 3DCP Flat Ribbed Beam foundation and the optimized 3DCP Short Flat Ribbed Beam foundation.

These life cycle indicators and trends can inform the future research and development of 3DCP technology for new onshore and offshore wind turbine support structures (e.g., foundations, towers, and offshore anchors) that minimize greenhouse gas emissions and energy usage.

Acknowledgements

The authors would like to thank Mr. Jason Cotrell and Dr. Gabriel Falzone at RCAM Technologies and Dr. Zhi-Yuan Cheng and Mr. Shashank Dholakia at WSP for providing information on the structural design process of the concrete printed foundations. This work was supported by California Energy Commission (No. EPC-19-007) and the US Department of Education GAANN Fellowship Program.

Data Availability Statement

The data that support the findings of this study are available from the corresponding author upon reasonable request.

References

1. P. Friedlingstein, M. O'Sullivan, M. W. Jones, et al., "Global Carbon Budget 2022," *Earth System Science Data* 14, no. 11 (2022): 4811–4900, https://doi.org/10.5194/essd-14-4811-2022.

2. D. Gilfillan and G. Marland, "CDIAC-FF: Global and National CO_2 Emissions From Fossil Fuel Combustion and Cement Manufacture: 1751–2017," *Earth System Science Data* 13, no. 4 (2021): 1667–1680, https://doi.org/10.5194/essd-13-1667-2021.

3. IPCC, *Climate Change 2014: Synthesis Report. Contribution of Working Groups I, II and III to the Fifth Assessment Report of the Intergovernmental Panel on Climate Change [Core Writing Team, R.K. Pachauri and L.A. Meyer (eds.)]* (IPCC, 2014).

4. R. Wiser, M. Bolinger, G. Barbose, et al., *2018 Wind Technologies Market Report* (U.S. Department of Energy, 2018).

5. R. Wiser, M. Bolinger, and Lawrence Berkely National Laboratory, *Land-Based Wind Market Report*, 2023rd ed. (U.S. Department of Energy, 2023), https://www.energy.gov/sites/default/files/2023-08/land-based-wind-market-report-2023-edition.pdf.

6. E. Lantz, O. Roberts, and K. Dykes, *Trends, Opportunities, and Challenges for Tall Wind Turbine and Tower Technologies* (NREL, 2017), https://www.nrel.gov/docs/fy17osti/68732.pdf.

7. J. Cotrell, S. Jenne, and S. Butterfield, *3D Concrete Printing Concept Could Solve Tall-Wind Dilemma* (Department of Energy, 2016), https://www.osti.gov/servlets/purl/1337883.

8. Hartman, L. *Wind Turbines: The Bigger, the Better* (U.S. Department of Energy, 2021). Energy.gov, https://www.energy.gov/eere/articles/wind-turbines-bigger-better.

9. WINDExchange, *WINDExchange: California Potential Wind Capacity Chart* (WINDExchange, 2015) https://windexchange.energy.gov/maps-data/14.

10. J. Zayas, M. Derby, P. Gilman, et al., *Enabling Wind Power Nationwide* (U.S. Department of Energy, 2015), https://www.energy.gov/sites/default/files/2015/05/f22/Enabling%20Wind%20Power%20Nationwide_18MAY2015_FINAL.pdf.

11. W. Musial, P. Spitsen, P. Duffy, et al., *Offshore Wind Market Report*, 2023rd ed. (U.S. Department of Energy, 2023), https://www.energy.gov/sites/default/files/2023-09/doe-offshore-wind-market-report-2023-edition.pdf.

12. ACI Innovation Task Group 9, *ACI ITG-9R-16 Report on Design of Concrete Wind Turbine Towers* (ACI, 2016).

13. H. Svensson, *Design of Foundations for Wind Turbines* (Lund University, 2010), https://www.byggmek.lth.se/fileadmin/byggnadsmekanik/publications/tvsm5000/web5173.pdf.

14. *Climate Change and the Production of Iron and Steel* (Worldsteel Association, 2021[Public policy paper]), https://worldsteel.org/wp-content/uploads/Climate-policy-paper-2021-1.pdf.

15. P. J. M. Monteiro, S. A. Miller, and A. Horvath, "Towards Sustainable Concrete," *Nature Materials* 16, no. 7 Article 7 (2017): 698–699, https://doi.org/10.1038/nmat4930.

16. F. Bos, R. Wolfs, Z. Ahmed, and T. Salet, "Additive Manufacturing of Concrete in Construction: Potentials and Challenges of 3D Concrete Printing," *Virtual and Physical Prototyping* 11, no. 3 (2016): 209–225, https://doi.org/10.1080/17452759.2016.1209867.

17. R. A. Buswell, W. R. Leal de Silva, S. Z. Jones, and J. Dirrenberger, "3D Printing Using Concrete Extrusion: A Roadmap for Research," *Cement and Concrete Research* 112 (2018): 37–49, https://doi.org/10.1016/j.cemconres.2018.05.006.

18. C. Gosselin, R. Duballet, P. Roux, N. Gaudillière, J. Dirrenberger, and P. Morel, "Large-Scale 3D Printing of Ultra-High Performance Concrete – A New Processing Route for Architects and Builders," *Materials & Design* 100 (2016): 102–109, https://doi.org/10.1016/j.matdes.2016.03.097.

19. A. Kazemian, X. Yuan, E. Cochran, and B. Khoshnevis, "Cementitious Materials for Construction-Scale 3D Printing: Laboratory Testing of Fresh Printing Mixture," *Construction and Building Materials* 145 (2017): 639–647, https://doi.org/10.1016/j.conbuildmat.2017.04.015.

20. V. Mechtcherine, F. P. Bos, A. Perrot, et al., "Extrusion-Based Additive Manufacturing With Cement-Based Materials – Production Steps, Processes, and Their Underlying Physics: A Review," *Cement and Concrete Research* 132 (2020): 106037, https://doi.org/10.1016/j.cemconres.2020.106037.

21. Y. Han, Z. Yang, T. Ding, and J. Xiao, "Environmental and Economic Assessment on 3D Printed Buildings With Recycled Concrete," *Journal of Cleaner Production* 278 (2021): 123884, https://doi.org/10.1016/j.jclepro.2020.123884.

22. S. Hou, Z. Duan, J. Xiao, and J. Ye, "A Review of 3D Printed Concrete: Performance Requirements, Testing Measurements and Mix Design," *Construction and Building Materials* 273 (2021): 121745, https://doi.org/10.1016/j.conbuildmat.2020.121745.

23. K. E. S. Jones and M. Li, "Life Cycle Assessment of Ultra-Tall Wind Turbine Towers Comparing Concrete Additive Manufacturing to Conventional Manufacturing," *Journal of Cleaner Production* 417 (2023): 137709, https://doi.org/10.1016/j.jclepro.2023.137709.

24. M. Bekaert, K. Van Tittelboom, and G. De Schutter, "Printed Concrete as Formwork Material: A Preliminary Study," in *Second RILEM International Conference on Concrete and Digital Fabrication*, eds. F. P. Bos, S. S. Lucas, R. J. M. Wolfs, and T. A. M. Salet (Springer International Publishing, 2020), 575–583, https://doi.org/10.1007/978-3-030-49916-7_59.

25. Y. Chen, Y. Zhang, Z. Liu, Y. Zhang, C. Liu, and B. Pang, "3D-Printed Concrete Permanent Formwork: Effect of Postcast Concrete Proportion on Interface Bonding," *Materials Letters* 344 (2023): 134472, https://doi.org/10.1016/j.matlet.2023.134472.

26. D. Zhang, G. Ma, J. Guan, L. Wang, and Q. Wang, "Cyclic Behavior of Unbonded Post-Tensioned Precast Segmental Concrete Columns Fabricated by 3D Printed Concrete Permanent Formwork," *Engineering Structures* 292 (2023): 116436, https://doi.org/10.1016/j.engstruct.2023.116436.

27. B. Zhu, B. Nematollahi, J. Pan, Y. Zhang, Z. Zhou, and Y. Zhang, "3D Concrete Printing of Permanent Formwork for Concrete Column Construction," *Cement and Concrete Composites* 121 (2021): 104039, https://doi.org/10.1016/j.cemconcomp.2021.104039.

28. C. Rebelo, A. Moura, H. Gervásio, M. Veljkovic, and L. Simões da Silva, "Comparative Life Cycle Assessment of Tubular Wind Towers and Foundations – Part 1: Structural Design," *Engineering Structures* 74 (2014): 283–291, https://doi.org/10.1016/j.engstruct.2014.02.040.

29. N. Stavridou, E. Koltsakis, and C. C. Baniotopoulos, "A Comparative Life-Cycle Analysis of Tall Onshore Steel Wind-Turbine Towers," *Clean Energy* 4, no. 1 (2020): 48–57, https://doi.org/10.1093/ce/zkz028.

30. H. Gervásio, C. Rebelo, A. Moura, M. Veljkovic, and L. Simões da Silva, "Comparative Life Cycle Assessment of Tubular Wind Towers and Foundations – Part 2: Life Cycle Analysis," *Engineering Structures* 74 (2014): 292–299, https://doi.org/10.1016/j.engstruct.2014.02.041.

31. J. P. Jensen, "Evaluating the Environmental Impacts of Recycling Wind Turbines," *Wind Energy* 22, no. 2 (2019): 316–326, https://doi.org/10.1002/we.2287.

32. E. Martínez, F. Sanz, S. Pellegrini, E. Jiménez, and J. Blanco, "Life Cycle Assessment of a Multi-Megawatt Wind Turbine," *Renewable Energy* 34, no. 3 (2009): 667–673, https://doi.org/10.1016/j.renene.2008.05.020.

33. A. Schreiber, J. Marx, and P. Zapp, "Comparative Life Cycle Assessment of Electricity Generation by Different Wind Turbine Types," *Journal of Cleaner Production* 233 (2019): 561–572, https://doi.org/10.1016/j.jclepro.2019.06.058.

34. Circular Concrete Pours: Tips on Pouring a Circular Foundation for a Grain Bin, *For Construction Pros* (For Construction Pros.com, 2021), https://www.forconstructionpros.com/concrete/article/21415346/curb-roller-manufacturing-circular-concrete-pours-tips-on-pouring-a-circular-foundation-for-a-grain-bin.

35. Locogen, (Director)*Locogen Wind Turbine Construction Timelapse* (Youtube.com, 2015), accessed October 16, 2023, https://www.youtube.com/watch?v=SBbBh5xZ1gQ.

36. www.ceasy.fr, A. C.CTE WIND, *Gravity Foundation* (CTE Wind International, n.d.) Retrieved October 11, 2023, from https://www.cte-wind.com/solution/standard-slab-foundation/.

37. RCAM Technologies and WSP USA, *Preliminary Tower and Foundation Design Report (EPC 19-007)* (California Energy Commission, 2022).

38. Viaintermedia.com, *Wind—Tree-Inspired Wind Turbine Foundation Could Reduce CO2 Emissions by 80%* (Renewable Energy Magazine, 2023), https://www.renewableenergymagazine.com/wind/treeinspired-wind-turbine-foundation-could-reduce-co2-20230606.

39. Modern Power Systems. *Two Emerging Innovations in Wind Turbine Foundation Design*. (NS Energy, 2021), https://www.nsenergybusiness.com/features/wind-turbine-foundation-design/.

40. J. E. Bowles, *Foundation Analysis and Design*, 5. ed., internat. ed. (McGraw-Hill, 1996).

41. ACI Committee 318, *ACI 318-19 Building Code Requirements for Structural Concrete* (ACI 318-19) and Commentary (ACI 318R-19) (ACI, 2019).

42. CSI, *SAP2000 Integrated Software for Structural Analysis and Design [Computer Software]* (Computers & Structures, Inc., n.d.).

43. ISO, *ISO 14040. Environmental Management – Life Cycle Assessment – Principles and Framework* (Geneva, Switzerland: International organization for standardization, 2006a).

44. ISO, *ISO 14044. Environmental Management – Life Cycle Assessment – Requirements and Guidelines* (Geneva, Switzerland: International organization for standardization, 2006b).

45. Office of Transportation and Air Quality. Assessment and Standards Division, *Median Life, Annual Activity, and Load Factor Values for Nonroad Engine Emissions Modeling* (United States Environmental Protection Agency, 2010).

46. G. Wernet, C. Bauer, B. Steubing, J. Reinhard, E. Moreno-Ruiz, and B. Weidema, "Ecoinvent Database Version 3 (Part I): Overview and Methodology," *The International Journal of Life Cycle Assessment*. 21 (2016): 1218–1230, https://doi.org/10.1007/s11367-016-1087-8.

47. C. P. Company, *EPD for Concrete Produced at 8 CalPortland California Facilities (NRMCAEPD: 20035)* (CalPortland Company, 2020), https://www.nrmca.org/wp-content/uploads/2020/08/CalportlandCaliforniaNRMCAEPD20035.pdf.

48. Megavind, *Strategy for Extending the Useful Lifetime of a Wind Turbine* (Megavind, 2016).

49. U.S. Department of Energy, *Wind Energy End-of-Service Guide* (Office of Energy Efficiency and Renewable Wind energy Technologies Office: WINDExchange, 2023), https://windexchange.energy.gov/end-of-service-guide.

50. H. Liu, C. Liu, Y. Wu, et al., "Hardened Properties of 3D Printed Concrete With Recycled Coarse Aggregate," *Cement and Concrete Research* 159 (2022): 106868, https://doi.org/10.1016/j.cemconres.2022.106868.

51. R. B. Singh and B. Singh, "Rheological Behaviour of Different Grades of Self-Compacting Concrete Containing Recycled Aggregates," *Construction and Building Materials* 161 (2018): 354–364, https://doi.org/10.1016/j.conbuildmat.2017.11.118.

52. J. Bowyer, S. Bratkovich, K. Fernholz, et al., *Understanding Steel Recovery and Recycling Rates and Limitations to Recycling* (Dovetail Partners, 2015), https://www.dovetailinc.org/report_pdfs/2015/dovetailsteelrecycling0315.pdf.

53. World Steel Association. *Life Cycle Inventory Methodology Report* (World Steel Association, 2017), https://worldsteel.org/wp-content/uploads/Life-cycle-inventory-methodology-report.pdf.

54. National Renewable Energy Laboratory. (2012). U.S. Life Cycle Inventory Database [dataset].

55. *SimaPro Database Industry 2.0 Library* (SimaPro, 2018) [dataset].

56. A. V. Rahul, M. K. Mohan, G. De Schutter, and K. Van Tittelboom, "3D Printable Concrete With Natural and Recycled Coarse Aggregates: Rheological, Mechanical and Shrinkage Behaviour," *Cement and Concrete Composites* 125 (2022): 104311, https://doi.org/10.1016/j.cemconcomp.2021.104311.

57. Z. Ahmed, A. Biffi, L. Hass, F. Bos, and T. Salet, "3D Concrete Printing—Free Form Geometries With Improved Ductility and Strength," in *Second RILEM International Conference on Concrete and Digital Fabrication*, eds. F. P. Bos, S. S. Lucas, R. J. M. Wolfs, and T. A. M. Salet (Springer International Publishing, 2020), 741–756, https://doi.org/10.1007/978-3-030-49916-7_74.

58. K. Kinomura, S. Murata, Y. Yamamoto, H. Obi, and A. Hata, "Application of 3D Printed Segments Designed by Topology Optimization Analysis to a Practical Scale Prestressed Pedestrian Bridge," in *Second RILEM International Conference on Concrete and Digital Fabrication*, vol. 28, eds. F. P. Bos, S. S. Lucas, R. J. M. Wolfs, and T. A. M. Salet (Springer International Publishing, 2020), 658–668, https://doi.org/10.1007/978-3-030-49916-7_66.

59. A. Rezaei, Y. Guo, J. Keller, and A. R. Nejad, "Effects of Wind Field Characteristics on Pitch Bearing Reliability: A Case Study of 5 MW

Reference Wind Turbine at Onshore and Offshore Sites," *Forschung im Ingenieurwesen* 87, no. 1 (2023): 321–338, https://doi.org/10.1007/s10010-023-00654-x.

60. H. L. Raadal, B. I. Vold, A. Myhr, and T. A. Nygaard, "GHG Emissions and Energy Performance of Offshore Wind Power," *Renewable Energy* 66 (2014): 314–324, https://doi.org/10.1016/j.renene.2013.11.075.

61. *System Advisor Model(2021.12.02), N.D[Computer software]* (National Renewable Energy Laboratory), accessed April 21, 2022, https://sam.nrel.gov.

62. C. Roux, K. Kuzmenko, N. Roussel, R. Mesnil, and A. Feraille, "Life Cycle Assessment of a Concrete 3D Printing Process," *The International Journal of Life Cycle Assessment* 28, no. 1 (2023): 1–15, https://doi.org/10.1007/s11367-022-02111-3.

Appendix A

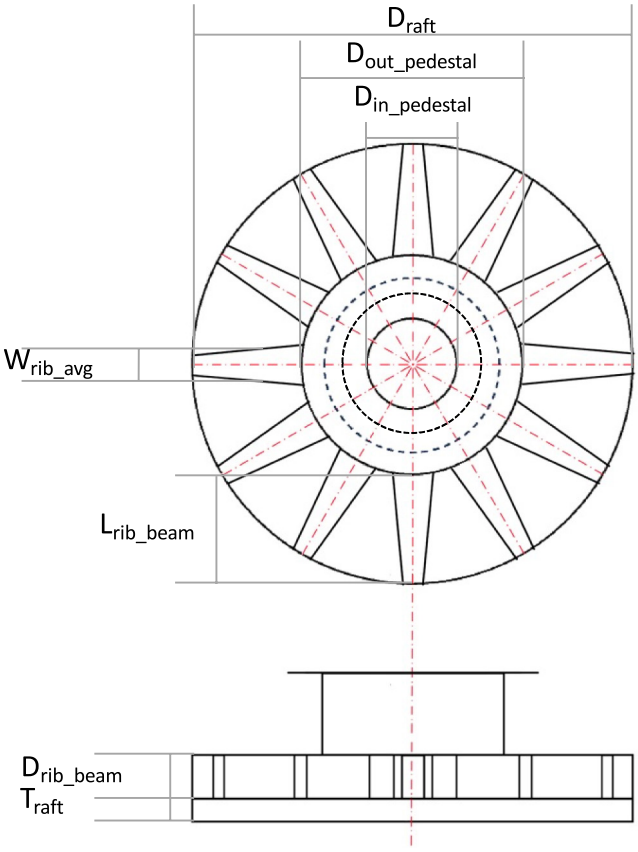

FIGURE A1 | Geometry of the 3DCP Flat Ribbed Beam foundation.

TABLE A1 Material inventory of each foundation with their corresponding SimaPro inventory selection, drawing from the USLCI, Ecoinvent 3, and Industry Data 2.0 databases.

Process or material	Quantity	Unit	Selected inventory process/emission
Conventional Circular foundation	1	p	
35 MPa ready-mix	1745.3	cu.yd	35 MPa Concrete CalPortland Mix 45EF6Z[a]
Rebar	176,715	lb	Steel rebar/GLO
Worker transportation	3.32E+03	pmi	Transport, passenger car, gasoline powered/personkm/RNA
Material transportation	3.19E+04	tkm	Transport, combination truck, short-haul, diesel powered, west/tkm/RNA
Concrete mixer	8.1	h	Machine operation, diesel, ≥ 74.57 kW, steady-state {GLO}
Concrete pump	8.1	h	Machine operation, diesel, ≥ 74.57 kW, high-load factor {GLO}
Conventional Tapered foundation	1	p	
35 MPa ready-mix	1327.6	cu.yd	35 MPa Concrete CalPortland Mix 45EF6Z[a]
Rebar	134,416	lb	Steel rebar/GLO
Worker transportation	3.32E+03	pmi	Transport, passenger car, gasoline powered/personkm/RNA
Material transportation	2.43E+04	tkm	Transport, combination truck, short-haul, diesel powered, west/tkm/RNA
Concrete mixer	6.2	h	Machine operation, diesel, ≥ 74.57 kW, steady-state {GLO}
Concrete pump	6.2	h	Machine operation, diesel, ≥ 74.57 kW, high load factor {GLO}
3DCP Flat Ribbed Beam foundation	1	p	
3D printed cement	4.25E+05	kg	11 ksi 3DCP concrete
35 MPa ready-mix	872.7	cu.yd	35 MPa Concrete CalPortland Mix 45EF6Z[a]
Rebar	115,160	lb	Steel rebar/GLO
Worker transportation	3.60E+03	pmi	Transport, passenger car, gasoline powered/personkm/RNA
Material transportation	2.05E+04	tkm	Transport, combination truck, short-haul, diesel powered, west/tkm/RNA
3D printer operation	5.62E+01	h	3DCP printer run time
Printer transport	5.55E+02	tkm	Transport, light commercial truck, diesel powered, west/tkm/RNA
Concrete mixer	4.1	h	Machine operation, diesel, ≥ 74.57 kW, steady-state {GLO}
Concrete pump	4.1	h	Machine operation, diesel, ≥ 74.57 kW, high load factor {GLO}
3DCP Short Flat Ribbed Beam	1	p	
3D printed cement	3.39E+05	kg	11 ksi 3DCP concrete
35 MPa ready-mix	872.7	cu.yd	35 MPa Concrete CalPortland Mix 45EF6Z[a]
Rebar	109,760	lb	Steel rebar/GLO
Worker transportation	3.60E+03	pmi	Transport, passenger car, gasoline powered/personkm/RNA
Material transportation	1.96E+04	tkm	Transport, combination truck, short-haul, diesel powered, west/tkm/RNA
3D printer operation	4.49E+01	h	3DCP printer run time
Printer transport	5.55E+02	tkm	Transport, light commercial truck, diesel powered, west/tkm/RNA
Concrete mixer	4.1	h	Machine operation, diesel, ≥ 74.57 kW, steady-state {GLO}
Concrete pump	4.1	h	Machine operation, diesel, ≥ 74.57 kW, high load factor {GLO}

[a]From CalPortland Company [47].

TABLE A2 Emission inventory used for 3D printer calculations.

Process or material	Quantity	Unit	Selected inventory process/emission
3DCP printer run time	1	h	
Robot ABB[a]	1	h	RoboticSystem

[a]Modeled using supplementary materials provided by [62] in "Supplementary file5" for a single hour use of one 6-axis 3D printer.

TABLE A3 Material inventory of modeled 78-MPa 3D printed concrete.

Process or material	Quantity	Unit	Selected inventory process/emission
78-MPa 3D printed concrete[a]	17,808.5	g	
Cement	8500	g	Cement, Portland {US}|market for
Sand	5000	g	Silica sand {GLO}|market for
Water	2650	g	Tap water {RoW}|tap water production, conventional treatment
Super plasticizer	145	g	Plasticizer, for concrete, based on sulfonated melamine formaldehyde {GLO}|market for
VMA	5	g	1-Butanol {RoW}|hydroformylation of propylene
Retarder	8.5	g	Plasticizer, for concrete, based on sulfonated melamine formaldehyde {GLO}|market for
Transport	—	tkm	Transport by weight taken from concrete, 50 MPa {GLO}|market for

aMasses of silica fume not included due to the material's status as a waste byproduct.

TABLE A4 | Summarized impacts of Conventional Circular, Circular Tapered, 3DCP Flat Ribbed Beam, and 3DCP Short Flat Ribbed Beam wind turbine foundations broken down by life cycle stage contributions.

	Ozone depletion	Global warming	Smog	Acidification	Eutrophication	Fossil fuel depletion	Carcinogenics	Noncarcinogenics	Respiratory effects	Ecotoxicity
3DCP Short Flat Ribbed Beam	**kg CFC-11 eq**	**kg CO_2 eq**	**kg O_3 eq**	**kg SO_2 eq**	**kg N eq**	**MJ surplus**	**CTUh**	**CTUh**	**kg PM2.5 eq**	**CTUe**
Materials	**1.16E−02**	**4.95E+05**	**2.64E+04**	**1.53E+03**	**3.19E+02**	**3.12E+05**	**1.01E−02**	**5.69E−02**	**2.07E+02**	**1.22E+06**
Transport	1.15E−07	2.74E+03	8.08E+02	3.19E+01	1.91E+00	5.75E+03	4.10E−05	3.95E−04	1.03E+00	7.64E+03
Construction	2.44E−04	2.17E+03	2.47E+02	1.09E+01	4.14E+00	4.37E+03	9.64E−05	8.16E−04	7.37E−01	1.89E+04
Use	NA	NA	NA	NA	NA	NA	NA	NA	NA	NA
End of life	1.39E−03	7.43E+03	2.17E+03	7.64E+01	−3.26E+00	2.68E+04	1.24E−05	3.85E−04	−2.63E+01	4.11E+03
Total	*1.32E−02*	*5.07E+05*	*2.96E+04*	*1.65E+03*	*3.22E+02*	*3.49E+05*	*1.03E−02*	*5.85E−02*	*1.83E+02*	*1.25E+06*
3DCP Flat Ribbed Beam										
Materials	**1.35E−02**	**5.40E+05**	**2.83E+04**	**1.64E+03**	**3.77E+02**	**3.37E+05**	**1.09E−02**	**6.20E−02**	**2.28E+02**	**1.35E+06**
Transport	1.19E−07	2.84E+03	8.39E+02	3.31E+01	1.98E+00	5.97E+03	4.26E−05	4.11E−04	1.07E+00	7.94E+03
Construction	2.49E−04	2.22E+03	2.50E+02	1.12E+01	4.90E+00	4.41E+03	1.10E−04	9.70E−04	7.97E−01	2.26E+04
Use	NA	NA	NA	NA	NA	NA	NA	NA	NA	NA
End of life	1.45E−03	7.75E+03	2.27E+03	7.97E+01	−3.46E+00	2.80E+04	1.21E−05	3.98E−04	−2.76E+01	4.18E+03
Total	*1.52E−02*	*5.52E+05*	*3.17E+04*	*1.76E+03*	*3.80E+02*	*3.75E+05*	*1.11E−02*	*6.38E−02*	*2.03E+02*	*1.39E+06*
Conventional Tapered										
Materials	**6.37E−03**	**4.83E+05**	**2.85E+04**	**1.68E+03**	**1.37E+02**	**3.27E+05**	**1.06E−02**	**5.60E−02**	**1.87E+02**	**1.06E+06**
Transport	1.16E−07	2.77E+03	8.17E+02	3.22E+01	1.93E+00	5.83E+03	4.15E−05	4.01E−04	1.01E+00	7.74E+03
Construction	3.41E−04	2.41E+03	2.77E+02	1.15E+01	1.50E+00	5.07E+03	5.42E−05	2.17E−04	6.81E−01	4.53E+03
Use	NA	NA	NA	NA	NA	NA	NA	NA	NA	NA
End of life	1.73E−03	9.27E+03	2.72E+03	9.57E+01	−3.77E+00	3.34E+04	1.96E−05	4.96E−04	−3.20E+01	5.56E+03
Total	*8.44E−03*	*4.98E+05*	*3.23E+04*	*1.82E+03*	*1.36E+02*	*3.71E+05*	*1.07E−02*	*5.71E−02*	*1.56E+02*	*1.08E+06*
Conventional Circular										
Materials	**8.37E−03**	**6.35E+05**	**3.75E+04**	**2.21E+03**	**1.80E+02**	**4.29E+05**	**1.39E−02**	**7.36E−02**	**2.46E+02**	**1.40E+06**
Transport	1.53E−07	3.65E+03	1.07E+03	4.24E+01	2.54E+00	7.66E+03	5.46E−05	5.27E−04	1.33E+00	1.02E+04

(Continues)

TABLE A4 | (Continued)

3DCP Short Flat Ribbed Beam	Ozone depletion kg CFC-11 eq	Global warming kg CO_2 eq	Smog kg O_3 eq	Acidification kg SO_2 eq	Eutrophication kg N eq	Fossil fuel depletion MJ surplus	Carcinogenics CTUh	Noncarcinogenics CTUh	Respiratory effects kg PM2.5 eq	Ecotoxicity CTUe
Construction	4.45E−04	2.85E+03	3.26E+02	1.33E+01	1.87E+00	6.00E+03	6.64E−05	2.41E−04	8.55E−01	5.09E+03
Use	NA	NA	NA	NA	NA	NA	NA	NA	NA	NA
End of life	2.27E−03	1.21E+04	3.56E+03	1.26E+02	−4.97E+00	4.37E+04	2.49E−05	6.45E−04	−4.21E+01	7.16E+03
Total	*1.11E−02*	*6.54E+05*	*4.24E+04*	*2.39E+03*	*1.79E+02*	*4.87E+05*	*1.41E−02*	*7.50E−02*	*2.06E+02*	*1.42E+06*

Note: Maximum values in each category are in bold, total values are in italics.

TABLE A5 | Summarized impacts of Conventional Circular, Circular Tapered, 3DCP Flat Ribbed Beam, and 3DCP Short Flat Ribbed Beam wind turbine foundations broken down by life cycle stage percentage contributions.

	Ozone depletion	Global warming	Smog	Acidification	Eutrophication	Fossil fuel depletion	Carcinogenics	Noncarcinogenics	Respiratory effects	Ecotoxicity
	kg CFC-11 eq	kg CO_2 eq	kg O_3 eq	kg SO_2 eq	kg N eq	MJ surplus	CTUh	CTUh	kg PM2.5 eq	CTUe
3DCP Short Flat Ribbed Beam										
Materials	**87.7%**	**97.6%**	**89.1%**	**92.8%**	**97.2%**	**89.4%**	**98.5%**	**97.3%**	**88.1%**	**97.5%**
Transport	0.0009%	0.5%	2.7%	1.9%	0.6%	1.6%	0.4%	0.7%	0.4%	0.6%
Construction	1.8%	0.4%	0.8%	0.7%	1.3%	1.3%	0.9%	1.4%	0.3%	1.5%
Use	NA	NA	NA	NA	NA	NA	NA	NA	NA	NA
End of life	10.46%	1.5%	7.3%	4.6%	−1.0%	7.7%	0.1%	0.7%	−11.2%	0.3%
3DCP Flat Ribbed Beam										
Materials	**88.8%**	**97.7%**	**89.4%**	**93.0%**	**97.3%**	**89.8%**	**98.5%**	**97.2%**	**88.6%**	**97.5%**
Transport	0.001%	0.5%	2.6%	1.9%	0.5%	1.6%	0.4%	0.6%	0.4%	0.6%
Construction	1.6%	0.4%	0.8%	0.6%	1.3%	1.2%	1.0%	1.5%	0.3%	1.6%
Use	NA	NA	NA	NA	NA	NA	NA	NA	NA	NA
°End of life	9.5%	1.4%	7.2%	4.5%	−0.9%	7.5%	0.1%	0.6%	−10.7%	0.3%
Conventional Tapered										
Materials	**75.5%**	**97.1%**	**88.2%**	**92.3%**	**95.0%**	**88.1%**	**98.9%**	**98.0%**	**84.7%**	**98.3%**
Transport	0.001%	0.6%	2.5%	1.8%	1.3%	1.6%	0.4%	0.7%	0.5%	0.7%
Construction	4.0%	0.5%	0.9%	0.6%	1.0%	1.4%	0.5%	0.4%	0.3%	0.4%
Use	NA	NA	NA	NA	NA	NA	NA	NA	NA	NA
End of life	20.5%	1.9%	8.4%	5.3%	−2.6%	9.0%	0.2%	0.9%	−14.5%	0.5%
Conventional Circular										
Materials	**75.5%**	**97.2%**	**88.3%**	**92.4%**	**95.0%**	**88.2%**	**99.0%**	**98.1%**	**84.7%**	**98.4%**
Transport	0.001%	0.6%	2.5%	1.8%	1.3%	1.6%	0.4%	0.7%	0.5%	0.7%
Construction	4.0%	0.4%	0.8%	0.6%	1.0%	1.2%	0.5%	0.3%	0.3%	0.4%
Use	NA	NA	NA	NA	NA	NA	NA	NA	NA	NA
End of life	20.5%	1.9%	8.4%	5.3%	−2.6%	9.0%	0.2%	0.9%	−14.5%	0.5%

Note: Maximum values in each category are in bold.

TABLE A6 | Material inventory of rotor and nacelle via Table 2 of "GHG emissions and energy performance of offshore wind power" [60].

Turbine NREL 5 MW (all values in tons per WT)	Rotor (hub and blades)	Nacelle	Tower structure	Sum	Ecoinvent processes used in the analyses
Steel	60	197	234[a]	490	Steel, converter, low-alloyed, at plant/RER U (rotor and nacelle), steel, low-alloyed, at plant/RER U (tower)
Aluminum		8	5[a]	13	Aluminum, primary, at plant/RER S
Electronics			4	4	Electronics for control units/RER U
Plastic			4[a]	4	Polyethylene terephthalate, granulate, bottle grade, at plant/RER U
Copper		32	2[a]	35	Copper, at regional storage/RER U
Oil			2[a]	2	Lubricating oil, at plant/RER U
Glass-reinforced plastic	50	2		53	Glass fiber–reinforced plastic, polyamide, injection molding, at plant/RER U

[a]Values not used in the material inventory of the hub/blades/nacelle subassemblies. The tower electronics are included because outfitting is not included in the original tower LCA.